Thermochimica Acta 473 (2008) 25–31

Contents lists available at ScienceDirect

Thermochimica Acta

journal homepage: www.elsevier.com/locate/tca

Study on thermal decomposition and combustion of insensitive explosive 3,3′-diamino-4,4′-azofurazan (DAAzF)

V.P. Sinditskii[a,*], M.C. Vu[a], A.B. Sheremetev[b], N.S. Alexandrova[b]

[a] Mendeleev University of Chemical Technology, 9 Miusskaya Square, 125047 Moscow, Russia
[b] N.D. Zilinskiy Institute of Organic Chemistry, Russian Academy of Science, Leninsky Prosp., 47, Moscow 117913, Russia

ARTICLE INFO

Article history:
Received 6 February 2008
Received in revised form 4 April 2008
Accepted 8 April 2008
Available online 16 April 2008

Keywords:
3,3′-Diamino-4,4′-azofurazan (DAAzF)
Burning rate
Thermal decomposition
Temperature profiles in the combustion waves
Decomposition mechanism

ABSTRACT

Thermal decomposition of an explosive with low sensitivity, 3,3′-diamino-4,4′-azofurazan (DAAzF), has been investigated under isothermal conditions at 200–320 °C using the thin-walled glass manometer of the compensation type. Changing the ratio of the sample weight to the vessel volume allowed us to measure the kinetic parameters of DAAzF decomposition predominantly in the solid state ($k = 5.0 \times 10^{11} \exp(-21{,}320/T)$, s^{-1}) and the gas phase ($k = 3.3 \times 10^{12} \exp(-21{,}020/T)$, s^{-1}). The kinetics of decomposition in solution ($k = 3.5 \times 10^{6} \exp(-14{,}070/T)$, s^{-1}) have also been measured. Based on the burning rate and thermocouple measurement data, rate constants of DAAzF decomposition in the molten layer at 600–800 °C have been derived from a condensed-phase combustion model ($k = 4.6 \times 10^{8} \exp(-16{,}680/T)$, s^{-1}), which is in a good agreement with kinetic data obtained in the solution at 235–260 °C. The mechanism of DAAzF thermolysis and combustion includes initial rupture of C–N bond between the azo-group and furazan ring with subsequent nitrogen evolution and decomposition of the heterocyclic ring. In the combustion wave, the heat release from decomposition of the stable furazan ring follows the heat release from azo-group decomposition, resulting in a distinct two-stage flame structure.

1. Introduction

3,3′-Diamino-4,4′-azofurazan (DAAzF) has become the subject of significant investigations in recent years due to its potential as an insensitive explosive [1–7]. DAAzF is also considered as a possible ingredient of solid [8] and fuel-rich propellants [9]. DAAzF cannot be initiated by laboratory impact drop tests, and yet it has in some aspects better explosive performances than 1,3,5-triamino-2,4,6-trinitrobenzene (TATB)—the standard of insensitive high explosives [3].

The thermal stability of DAAzF is also attractive, with the onset temperature of the exotherm in DSC at 315 °C, which is comparable to that of hexanitrostilbene (HNS), yet DAAzF is also a better explosive performer than HNS [3]. However, studies reported for DAAzF thermal stability are limited to DSC data only. The only kinetic data of DAAzF thermal decomposition ($E = 336.8$ kJ mole^{-1}, $A = 10^{26.4}$ s^{-1}) have been obtained in non-isothermal conditions by means of DSC [10,11], and to all appearances are characteristic of a total process of DAAzF decomposition in both solid and gas phases accompanied by evaporation, rather than characteristic of the DAAzF breaking bonds strength. Furthermore, there are different opinions about the thermal stability of DAAzF. Thus, according to reference [8], DAAzF gave over 5 ml of gas per gram in the vacuum thermal stability test (VTS test, 100 °C, 48 h), which is unacceptable for a propellant ingredient. At the same time, according to Chinese researchers, DAAzF gave only 0.45 ml of gas per gram [10] or 0.26 ml g^{-1} [11] in the VTS test, which is quite satisfactory.

The purpose of the present work was to investigate DAAzF decomposition in different states of the material using an isothermal method. A study of thermal decomposition was accompanied by thermocouple-aided measurements in the combustion wave of DAAzF that allowed determination of the surface temperatures and, as a result, derivation of DAAzF decomposition reaction rates in a high-temperature interval characteristic of DAAzF combustion (600–800 °C).

2. Experimental

2.1. Preparation

3,3′-Diaminoazofurazan was synthesized by methods published elsewhere [12] as a dark-orange crystalline solid. Analysis confirmed the assigned structure. ^{1}H NMR (DMSO-d_6) δ 6.89 (s, 4H); ^{13}C NMR (DMSO-d_6) δ 150.4, 155.6. Anal. Calcd. for $C_4H_4N_8O_2$ (196.13): C 24.48, H 2.06, N 57.14. Found C 24.44, H 2.09, N 57.11.

* Corresponding author.
E-mail address: vps@rctu.ru (V.P. Sinditskii).

0040-6031/$ – see front matter © 2008 Elsevier B.V. All rights reserved.
doi:10.1016/j.tca.2008.04.004

2.2. Decomposition study

Manometric experiments were carried out in thin-walled glass manometers of the compensation type (the glass Bourdon gauge) at 200–320 °C. A sample of DAAzF (from 5 to 140 mg, depending on a type of experiment) was loaded in a glass manometer of 10–50 cm^3 volume. The device was evacuated to 10^{-2} mmHg, then it was sealed and immersed in a thermostatted Wood's metal bath. The temperature in the bath was maintained with an accuracy of ±0.5 °C. The pressure of the gases evolved in the experiments was measured with an accuracy of ±1 mmHg, which was then converted to gas volume at normal conditions, and the rate of gas evolution was then evaluated. The rate constant was calculated as a ratio of the initial gas evolution rate to the final volume of gases. In the case of experiments in solution, a sample of 2–6 mg DAAzF was admixed with 200 mg hexachlorobenzene and placed in a glass manometer with ~12 cm^3 volume.

2.3. Combustion study

Burning rates were measured in a constant-pressure window bomb of 1.5 l volume in the 0.6–15 MPa pressure interval. Samples to be tested were prepared as pressed cylinders of 0.90–0.95 of the theoretical maximum density (TMD) (1.728 g cm^{-3} [8]) confined in transparent acrylic tubes of 7 mm i.d. Prior to pressing, the material was thoroughly comminuted in order to produce samples with a minimum possible pore size, thus minimizing the possibility of flame propagation between particles.

Temperature profiles in the combustion wave were measured using fine thermocouples. The thermocouples were welded from 80%W + 20%Re and 95%W + 5%Re wires 25 μm thick followed by rolling in bands 5–7 μm thick. The thermocouple signal was recorded with a Pico ADC 216 digital oscilloscope.

2.4. Analysis

The condensed combustion and decomposition products were analyzed with a Nicolet Magna Fourier transform spectrometer, thin-layer, gas and liquid (Millikhrom-4) chromatography.

Thermodynamic calculations were performed with the use of the "REAL" computer simulation of chemical equilibrium code [13].

3. Results and discussion

3.1. Thermal decomposition of DAAzF

The first experiments on thermal decomposition of DAAzF under isothermal conditions were carried out at a loading density of ~10 mg cm^{-3} (the ratio of the sample weight to the vessel volume, m/V) in the temperature interval of 280–310 °C. Curves of the gas release have a shape typical of saturation conditions (Fig. 1). The rate constants calculated as a ratio of the initial gas evolution rate to the final volume of gases are presented in Fig. 2 and Table 1. In the ln k *vs.* reciprocal temperature coordinates, the experimental points fall on a straight line described by the following equation: $k(\text{in s}^{-1}) = 7.8 \times 10^{20} \exp(-32{,}680/T)$. As seen from Fig. 2, the kinetic parameters obtained (curve 1) prove to be quite close to those observed in the DSC experiments (curve 5) [10].

The observed activation energy (271.5 kJ $mole^{-1}$) is very high and can be explained by the fact that the kinetic parameters of DAAzF thermal decomposition in the solid phase are distorted by decomposition reactions in the gas phase, which role increases with temperature. Along with a condensed residue observed at the bottom of the vessel after the experiment is finished, a thin brownish film on the inner wall of the manometer remains, indicating the existence of gas-phase decomposition. Assuming that onset pressures in the glass Bourdon gauge are produced as a result of initial substance sublimation only, it is possible to evaluate the temperature dependence of vapor pressure above solid DAAzF. In the temperature range of 280–310 °C, the initial pressures follow the equation ln P (P in atm) = 18.61–11,960/T. The enthalpy of sublimation for DAAzF derived from it is 99.6 kJ $mole^{-1}$.

Knowing the DAAzF vapor pressure, it is easy to calculate the portion of the substance coming into the gas phase during our experiments at m/V ~10 mg cm^{-3}. It changes from 13 to 60% in the interval of 280–310 °C. Therefore, the kinetics parameters obtained

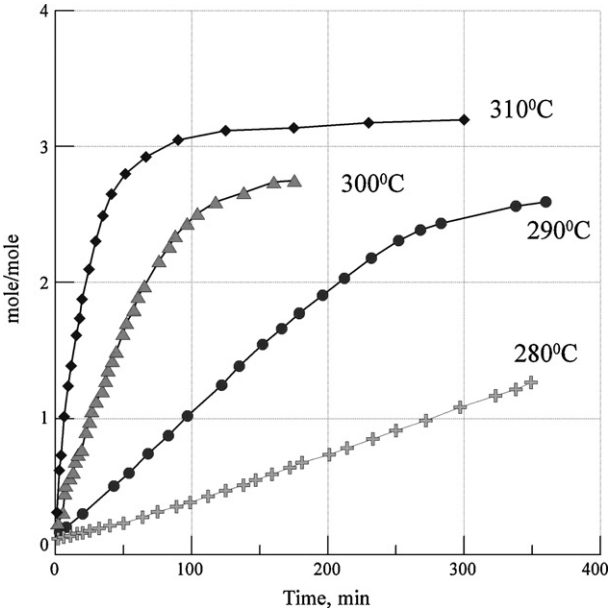

Fig. 1. Curves of the gas release from decomposition of DAAzF at m/V ~10 mg cm^{-3} and different temperatures.

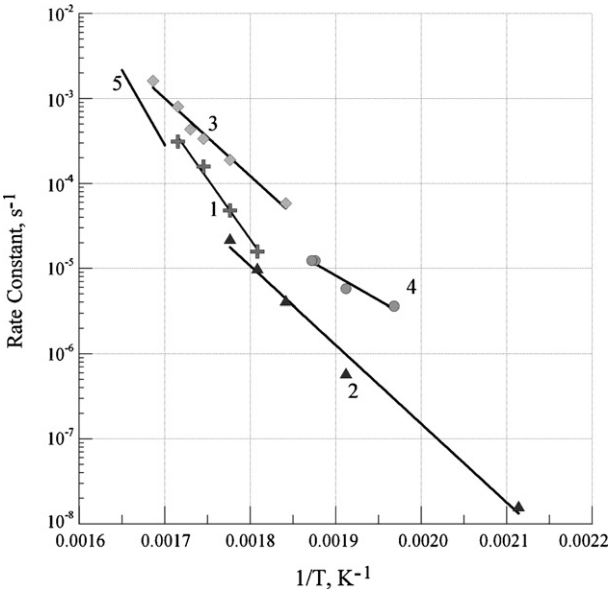

Fig. 2. The rate constants of DAAzF decomposition at different m/V (mg cm^{-3}): ~10 (1), ~100 (2), 0.5–5.6 (3) in comparison with the rate constants of the DAAzF decomposition in the solution (4) and data from Ref. [10] (5).

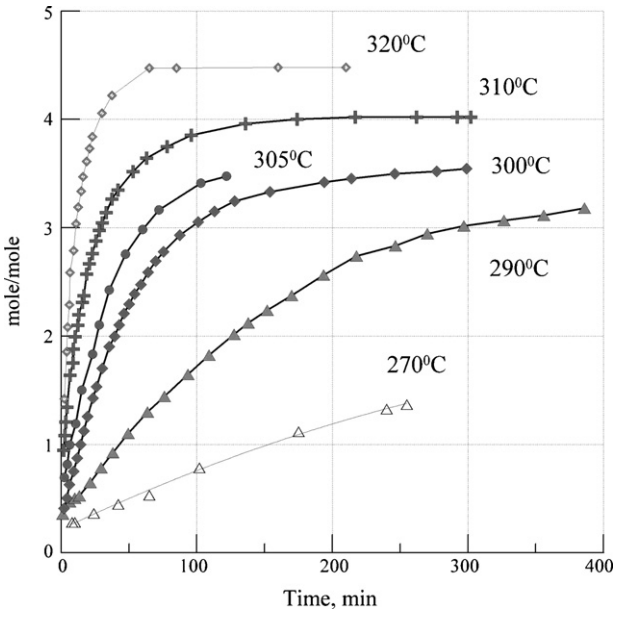

Fig. 3. Curves of the DAAzF gas release from decomposition in the gas phase (at $m/V = 0.5–5.6\,mg\,cm^{-3}$) at different temperatures.

are characteristic of the total process and are not fundamental values.

Taking into account the vapor pressure data obtained, decomposition of DAAzF has been studied in both the solid and gas phases. The gas-phase decomposition experiments were carried out at a loading density of $0.5–5.6\,mg\,cm^{-3}$ in the temperature interval of 270–320 °C. In this case, the only condensed residue after decomposition of DAAzF was a brownish film on the inner wall of the device. Typical curves of the gas released in decomposition of 1 mole of DAAzF are presented in Fig. 3. Rate constants are derived from the gas pressure, which can be described by the equation $P = P_0(1 - \exp^{-kt}) + P_\infty \exp^{-kt}$, where P_0 and P_∞ are an initial vapor pressure and final pressure of decomposition products, respectively. The kinetics of the gas-phase decomposition appeared to correspond to a first reaction order, at least up to 80% decomposition. In $\ln k$ *vs.* reciprocal temperature coordinates, the experimental points fall on a straight line described by the following equation: $k(\text{in } s^{-1}) = 3.3 \times 10^{12} \exp(-21{,}020/T)$ (Fig. 2, curve 3).

DAAzF thermal decomposition experiments in the solid state were carried out at the considerably higher loading density, $100\,mg\,cm^{-3}$, and reduced temperatures, 200–290 °C, to diminish the influence of gas-phase decomposition. The portion of the substance occurring in the gas phase at all temperatures studied was not more than 5% of total sample. The final gas volume after cooling to room temperature allowed estimation of the degree of DAAzF decomposition, which was usually less than 10%. There were almost no condensed decomposition products found upon cooling, and chromatographic analysis of the gaseous decomposition products indicated only nitrogen.

The decomposition of DAAzF under these conditions occurs at a constant rate. The temperature dependence of the rate constant is described by the following equation: $k = 5.0 \times 10^{11} \exp(-21{,}320/T)$, s^{-1} (Fig. 2, curve 2). Values of the activation energy of decomposition in both phases are close to each other (174.7 and 177.4 kJ $mole^{-1}$ in the gas and solid phase, respectively), but the rate of decomposition in the solid state is 10 times less (Table 1).

Comparison of the rate constants for DAAzF decomposition obtained under isothermal conditions with those obtained in DSC experiments shows that DSC kinetics data describe the cumulative process of DAAzF decomposition in both gas and solid phases (Fig. 2).

The full decomposition produces 4 mole of gases per mole of DAAzF (310 °C) at $m/V = 0.5–5.6\,mg\,cm^{-3}$ (Fig. 3) and 3.2 mole/mole at $m/V = 10\,mg\,cm^{-3}$ (Fig. 1). It is most likely that such a difference in the quantities of gaseous decomposition produces indicates different DAAzF decomposition mechanisms in gas and condensed phases.

Decreasing the temperature at which the experiment is conducted results in a regular decrease in the amount of gases evolved. This behavior can be explained by the fact that the vapor pressures of the condensed products formed during decomposition decrease as the temperature falls. This assumption is supported by the observation that the fraction of gases that condense upon cooling to room temperature decreases also with decreasing of experiment temperature, giving close values of 2.10–2.18 mole of noncondensable gases per mole of DAAzF. Cooling the remaining gases to low temperatures, from 0 to −195 °C, resulted in condensation of 45–46% gases that might be connected with condensation of gaseous CO (and CO_2). Remaining 55–56% of noncondensable gases are most likely nitrogen. In the case of gas-phase decomposition the content of nitrogen remains the same, but content of CO and CO_2 increases.

A gas chromatographic analysis of the decomposition products ($m/V = 10\,mg\,cm^{-3}$, 310 °C, full decomposition) also indicated the main gas products to be CO and nitrogen (together they constitute 96.22% in the ratio of 1:1.26) with a small impurity of CO_2 (3.6%) and N_2O (0.2%). HCN was practically absent in the composition of noncondensable gases. The CO/N_2 ratio proved to be very

Table 1
The kinetic parameters of DAAzF thermal decomposition in the solid, liquid and gas phases

Temperature (°C)	k (s^{-1}, at $m/V \sim 10\,mg/cm^3$)	k (s^{-1}, solid)	k (s^{-1}, liquid)	k (s^{-1}, gas)
200		1.62E−08		
235			3.62E−06	
250		5.93E−07	8.70E−06	
260			1.34E−05	
260			1.41E−05	
270		4.19E−06		5.83E−05
280	1.26E−05	1.01E−05		
290	3.80E−05	2.25E−05		
290				1.89E−04
300	1.20E−04			3.35E−04
305				4.33E−04
310	2.68E−04			7.99E−04
320				1.61E−03
Equation	$10^{20.89} \exp(-32{,}680/T)$	$10^{11.7} \exp(-21{,}320/T)$	$10^{6.54} \exp(-14{,}070/T)$	$10^{12.52} \exp(-21{,}020/T)$
Coefficient of determination	0.990	0.989	0.944	0.980

close to that observed during fast pyrolysis at 350–400 °C in the T-jump/FTIR spectroscopy experiments (1:1.44) [14], in which very little NO, NO_2, and N_2O was practically observed in the decomposition products. However, in contrast to our data, a large amount of HCN is formed in flash pyrolysis according to Beal [14]. This discrepancy can be explained by assuming that FTIR spectroscopy actually showed the presence of CN-group in some CN-containing product that was different from HCN and was condensed at room temperature.

Indeed, the condensed residue after DAAzF decomposition was found by thin layer and liquid chromatography to consist of two main products, one of them being identified as a dimer of cyanamide, dicyandiamide. In addition, liquid chromatography showed traces of a trimer of cyanamide, melamine.

According to our DSC data and the data of Li et al. [10], DAAzF begins to melt at 326 °C. The decomposition of liquid DAAzF cannot be studied by the manometric technique at temperatures higher than the melting temperature because of very high rates of decomposition. Therefore, decomposition of DAAzF in the liquid phase was studied at lower temperatures by using DAAzF in solution. Stable nitroaromatic compounds such as dinitrobenzene are usually used as solvents in such cases. However, in the case of DAAzF this solvent was inapplicable, since it reacted with DAAzF or with its decomposition products. Kinetic parameters of DAAzF decomposition in the liquid phase have been successfully obtained from decomposition of solutions of 1 and 2% DAAzF in hexachlorbenzene (HCB). In the temperature interval 235–260 °C, the temperature dependence of the rate constant is described by the following equation: $k = 3.5 \times 10^6 \exp(-14{,}070/T)$, s^{-1} (Fig. 2, curve 4). The rate of decomposition in the liquid state is very close to that in the gas phase, but the value of activation energy of decomposition in the liquid state is significantly less (117.2 kJ $mole^{-1}$).

A comparison of the rate constants of solid-phase decomposition of DAAzF with another explosive of low sensitivity, 5-nitro-1,2,4-triazol-3-one (NTO) [15], and with HMX [16], obtained with the same experimental technique, is presented in Fig. 4. It is seen from Fig. 4 that DAAzF is considerably more stable than solid NTO and HMX at temperatures below 220 °C.

A preliminary study of DAAzF combustion showed that at low pressures, the burning rate was governed by the condensed-phase

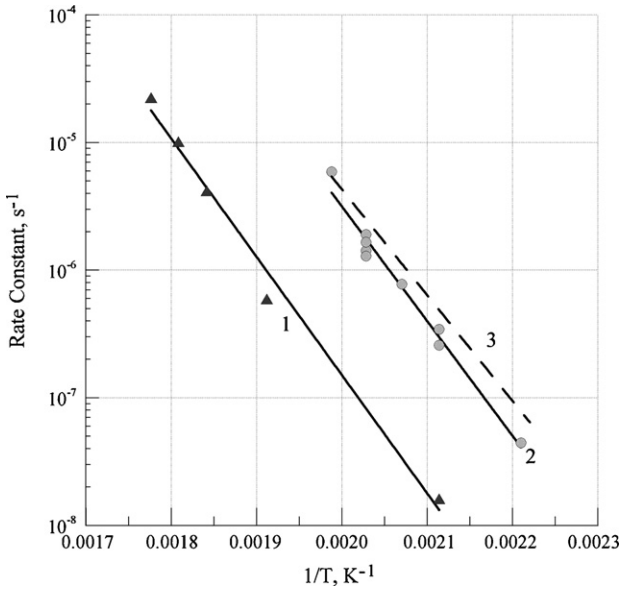

Fig. 4. Comparison of decomposition rate constants of solid DAAzF (1), NTO (2) and HMX (3), obtained by the same experimental technique.

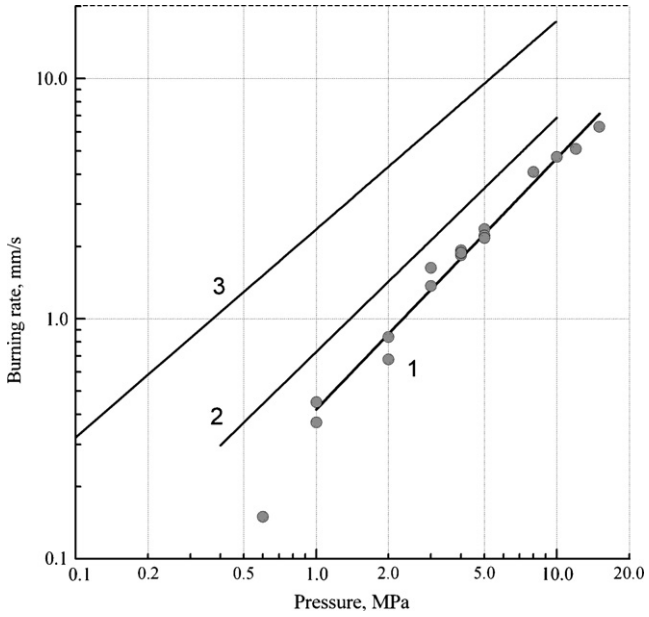

Fig. 5. Comparison of burning rates of DAAzF (1), NTO (2), and HMX (3).

chemistry. This may allow determination of DAAzF decomposition rate constants in the melt under combustion condition, i.e., in the high-temperature interval of 600–800 °C. For this purpose, it is necessary to know not only DAAzF burning rates, but surface temperatures as well.

3.2. Burning behavior and flame structure of DAAzF

DAAzF in the form of samples pressed into acrylic tubes of 7 mm diameter can sustain stable combustion at pressures above 0.6 MPa. The burning rate measured at 0.6 MPa (0.15 mm s^{-1}) is not considered in the discussion below because the burning is unstable. At 1 MPa DAAzF burns stably, and the burning is accompanied by formation of copious yellow smoke and solid residue inside the tubes. The burning rate at 10 MPa is only 4.7 mm s^{-1}, which is about 4 times slower than the burning rate of HMX and is comparable to the burning rate of NTO (Fig. 5). The DAAzF burning rate–pressure dependence is expressed as $r_b = 0.419p^{1.046}$, mm s^{-1} for the pressure interval of 1–15 MPa.

Temperature profiles in the DAAzF combustion wave were obtained at pressures of 1, 2, 4, and 5 MPa (Fig. 6). At all the pressures, temperature profiles demonstrated the presence of a region between surface and flame with a weak growth of temperature. At 1 MPa, the thermocouple did not show a temperature rise above the surface at a distance as long as ~1 mm. The temperature above the surface before ignition of the gas flame increases from 963 to ~1100 K (Table 2). As seen from Fig. 6, the appearance of the gas flame does not exert any effect on the DAAzF burning rate at pressures up to 5 MPa.

The maximum flame temperature is reached 1400–1450 °C at 5 MPa. It is much lower than the calculated adiabatic temperature (Table 2). It was shown earlier [17] that the incompleteness of heat release in the combustion of furazans is caused by formation of high-energy products. The furazan ring decomposition usually results in formation of nitrile and nitriloxide derivatives [18], isomerisation of the latter to isocyanate being the main heat release reaction during burning of furazan compounds. The difference between the maximum measured temperature and the calculated adiabatic temperatures amounts to ~835 K, which corresponds to 280 kJ $mole^{-1}$, assuming the average specific heat to

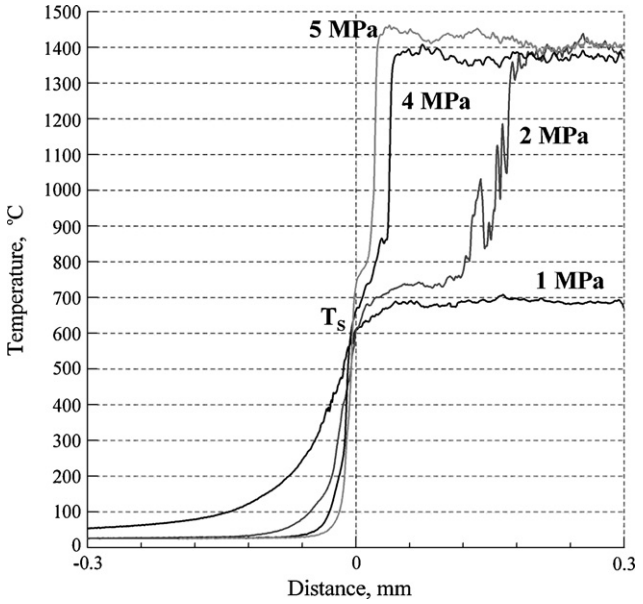

Fig. 6. Typical temperature profiles for DAAzF recorded at 1, 2, 4, and 5 MPa.

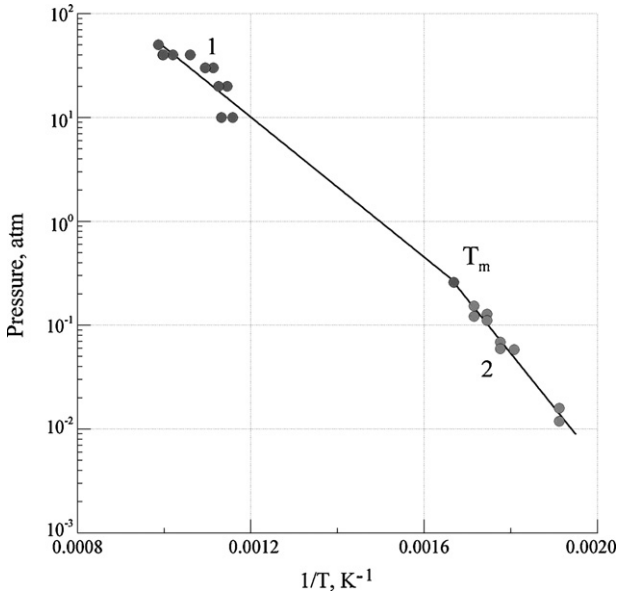

Fig. 7. Vapor pressure as a function of reciprocal temperature: DAAzF surface temperature (1) and initial pressures in DAAzF decomposition in glass Bourdon gauges (2).

be 1.67 kJ kg^{-1} K^{-1}. This value is close to the enthalpy of formation of two CN-fragments: ΔH_f° (HCN, gas) = 130.54 kJ mole^{-1} [19], ΔH_f° (C_2N_2, gas) = 308.95 kJ mole^{-1} [19], or ΔH_f° (H_2NCN, gas) = 130 kJ mole^{-1} (calculated).

The maximum measured temperature above the surface before the gas flame ignites is ~1100 K, which corresponds to a heat effect due to reactions in the melt of 360–376 kJ mole^{-1}, taking the average specific heat in this temperature interval as 1.67 kJ kg^{-1} K^{-1}.

The surface temperature in the pressure interval of 1–5 MPa ranged from 873 K (600 °C) to 1028 K (755 °C). The surface temperature in the interval of 1–5 MPa can be described by the following equation: $\ln P = -7759/T + 11.62$ (P in atm) (Fig. 7). The above dependence yields a DAAzF heat of evaporation of 60.7 kJ mole. The heat of sublimation of DAAzF derived from the temperature dependence of vapor pressure in the decomposition experiments is higher (99.6 kJ mole^{-1}), since it includes the heat of melting.

Based on one-dimensional conductive heat transfer analysis, the thermal diffusivity of molten DAAzF may be evaluated from the temperature distribution in the condensed phase. A plot of $\ln(T - T_0)/(T_s - T_0)$ *vs.* distance yields a straight line with the slope r_b/χ. At temperatures below 600 K, the thermal diffusivity of molten DAAzF is equal to $(1.4 \pm 0.3) \times 10^{-7}$ m^2 s^{-1}.

Combustion of DAAzF at 1 MPa leads to formation of a condensed yellow-brown residue amounting to about 37–42% of the initial sample weight. It corresponds almost quantitatively to the amount of cyanamide that might be formed in the decomposition of DAAzF. According to liquid chromatography analysis, the residue consists of a cyanamide condensation product, dicyandiamide, with an admixture of melamine and an unknown product, the nature of which is the same as in the decomposition experiments. IR-spectroscopy data of the residue show wide strong bands 3441, 3333, and 3157 cm^{-1} (νN–H), band 2168 cm^{-1} (νC≡N), and absorbance in the range of 1500–1650 cm^{-1} (δNH_2 and νC=N).

The heat flux from the gas to the surface at pressures at least up to 5 MPa is negligible, which consideration of the condensed-phase chemistry the determining factor in the combustion of DAAzF. Rate constants of the leading combustion reaction in the pressure range of 1–15 MPa can be obtained from the Zeldovich expression [20] for the mass burning rate (m), based on a dominant role of the condensed-phase chemistry:

$$m = \sqrt{\frac{2\rho^2 \chi Q}{c_p(T_s - T_0 + L_m/c_p)^2} \left(\frac{RT_s^2}{E}\right) A\, e^{-E/RT_s}}$$

where A is preexponential factor, E is activation energy, T_s and T_0 are surface and initial temperature, respectively. The average specific heat (c_p), thermal diffusivity (χ), and density of sample (ρ) were taken as 1.67 kJ kg^{-1} K^{-1}, 1.4×10^{-7} m^2 s^{-1}, and 1.67 g cm^{-3}, respectively. The heat of reaction in the melt, Q, was taken as 1841 J g^{-1} (360 kJ mole^{-1}), and the heat of melting, L_m (38.9 kJ mole^{-1} or 196.7 J g^{-1}) was obtained as the difference between the heat of sublimation, 99.6 kJ mole^{-1}, and the heat of evaporation, 60.7 kJ mole^{-1}.

As seen in Fig. 8, kinetic parameters of DAAzF decomposition derived from the combustion model, $k = 4.6 \times 10^8 \exp(-16{,}680/T)$, s^{-1} are in a good agreement with the experimental rate constants of DAAzF decomposition in the solution at low temperatures. Using rate constants of DAAzF decomposition derived from the combustion model in the temperature interval of 600–800 °C

Table 2
Characteristic temperatures in the combustion wave of DAAzF

Pressure (MPa)	Surface temperature, T_s (K)	Maximum temperature above the surface (K)	Maximum flame temperature, T_f (K)	Adiabatic flame temperature (K)
1	873 ± 11	963 ± 15	–	2550
2	881 ± 11	1003 ± 15	1655 ± 35	2554
3	906 ± 11	1100 ± 40	1650 ± 35	2556
4	982 ± 28	1135 ± 25	1645 ± 35	2558
5	1028 ± 35	1088 ± 35	1675 ± 20	2558

and data on the DAAzF decomposition in the solution at low temperatures, one can easily calculate the kinetics of DAAzF decomposition in the expanded temperature interval (250–800 °C): $k = 4.1 \times 10^8 \exp(-16{,}570/T)$, s^{-1} (coefficient of determination, 0.999). The activation energy of DAAzF decomposition in the liquid state in this temperature interval is 137.8 kJ mole^{-1}.

3.3. A mechanism of DAAzF thermal decomposition and combustion

Since the only gaseous product formed early in the decomposition of DAAzF proved to be nitrogen, it can be suggested that homolysis of the C–N bond between the furazan ring and the azo-group is the most probable initial step of unimolecular decomposition. As a result, a molecule of bis(diaminofurazanyl) can be formed. A similar transformation of azobenzenes is well known [21], but it was not observed previously in the chemistry of azofurazans. The heat effect of this reaction may be estimated as ~209 kJ mole^{-1}. However, as was already mentioned, the thermal effect of reaction in the melt amounts to 360–376 kJ mole^{-1} according to the thermocouple measurements. Hence, it is possible to assume that some further destruction of the furazan ring takes place, along with formation of bis(diaminofurazanyl) in the melt after loss of nitrogen. According to Teles and Maier [22], in pyrolysis at 500 °C through a quartz tube packed with quartz wool, 3,4-diaminofurazan produces a mixture of aminoisocyanate, cyanamide, isocyanic acid, and hydrogen cyanide with small amounts of carbon monooxide, carbodiimide and ammonia. A probable intermediate in this reaction is nitrile oxide. Therefore, it is possible to propose that DAAzF (and bis(diaminofurazanyl) also) can decompose to give cyanamide, aminonitrile oxide (presumably in approximately equal amounts), and cyanonitrile oxide. In order for the heat effect of the reaction to correspond to the measured heat release in the melt, it is necessary to suppose that one of the nitrile oxides turns into isocyanate:

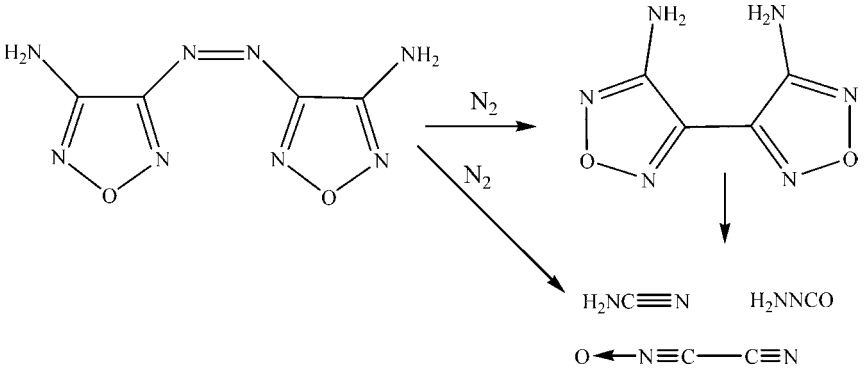

The further decomposition of cyanonitrile oxide to NCN radical and CO, and subsequent transformation of NCN and aminoisocyanate to 5-amino-1,2,4-triazol-3-one results in the final decomposition products:

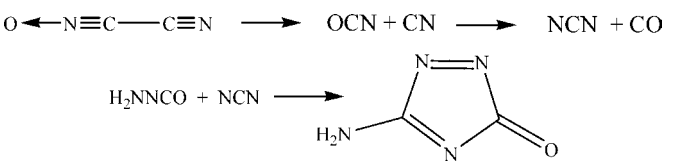

The heat effect of DAAzF decomposition reaction to CO, N_2, cyanamide, and aminotriazolone may be estimated as ~500–545 kJ mole^{-1}, which is in a good agreement with the maximum heat released in combustion (calculated from maximum measured flame temperatures). Condensation of cyanamide to solid dicyandiamide and melamine most likely occurs far from the gas reaction zone; otherwise, DAAzF flame temperatures would be significantly higher. It is necessary to note that no direct evidence for formation of aminotriazolone could be found. The proposed scheme allows us to explain the formation of about 2 mole of gases (CO/N_2) from decomposition of one mole of DAAzF.

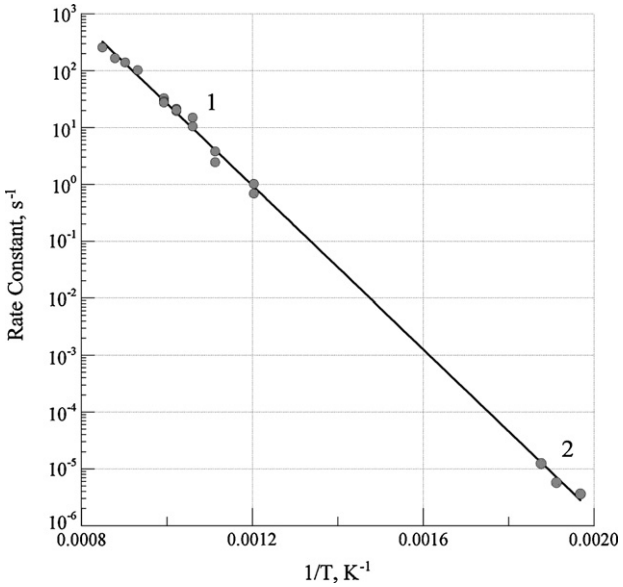

Fig. 8. Comparison of rate constants in a wide temperature interval: rate constants of the leading reaction in DAAzF combustion (1, points and line) and rate constants of the DAAzF decomposition in the solution (2, points).

4. Conclusions

The kinetic data obtained in DAAzF decomposition and the DAAzF combustion study were indicative of very similar activation energies of 174–176 kJ mole^{-1} in the gas and solid phases of the material and a significantly lower activation energy of 138 kJ mole^{-1} in the liquid phase. A comparison of the rate constants of solid-phase decomposition of DAAzF, another explosive of low sensitivity, 5-nitro-1,2,4-triazol-3-one (NTO), and HMX, obtained by using the same experimental technique, shows that DAAzF is considerably more stable in the solid state than NTO and HMX.

A mechanism of DAAzF thermolysis and combustion includes initial rupture of C–N bond between azo-group and furazan cycle

with subsequent nitrogen loss and decomposition of the heterocyclic ring. In the combustion wave, heat release from azo-group decomposition is followed by the heat release from decomposition of a stable furazan ring, resulting in a distinct two-stage flame structure in burning.

Acknowledgments

The authors would like to acknowledge Dr. Vera P. Shelaputina, Dr. Sergei P. Smirnov for their assistance in conducting the thermolysis and valuable remarks, Dr. Ruth Doherty for help in editing and valuable remarks and discussion.

References

[1] A.B. Sheremetev, V.O. Kulagina, L.V. Batog, O.V. Lebedev, I.L. Yudin, T.S. Pivina, V.G. Andrianov, I.B. Starchenkov, Proceedings of the 22nd International Pyrotechnics Seminar, July 15–19, 1996, Colorado, USA, 1996, pp. 377–388.
[2] M.A. Hiskey, D.E. Chavez, D.L. Naud, S.F. Son, H.L. Berghout, C.A. Bolme, Proceedings of the 27th International Pyrotechnics Seminar, July 16–21, 2000, Colorado, USA, 2000, pp. 3–14.
[3] D. Chavez, L. Hill, M. Hiskey, S. Kinkead, J. Energetic Mater. 18 (2000) 219–236.
[4] A.B. Sheremetev, V.O. Kulagina, N.S. Aleksandrova, All-Russian Conference "Energy Condensed Systems", October 28–31, 2002, Chernogolovka, Moscow-Yanus'K, 2002, p. 106.
[5] M.A. Hiskey, D.E. Chavez, R.L. Bishop, J.F. Kramer, S.A. Kinkead, US Patent 6,358,339 (March 19, 2002).
[6] A.B. Sheremetev, N.S. Aleksandrova, V.O. Kulagina, All-Russian Scientific-Engineering Conference "Modern Problems of Applied Chemistry", November 21–22, 2003, Kazan, Russia, 2003, pp. 213–214.
[7] A.B. Sheremetev, All-Russian Scientific-Engineering Conference "Modern Problems of Applied Chemistry", December 22–24, 2004, Kazan, Russia, 2004, pp. 282–289.
[8] L.F. Cannizzo, R.S. Hamilton, T.K. Highsmith, A.J. Sanderson, B.A. Zentner, AFRL-PR-ED-TP-1999-0207, 1999, 13 pp.
[9] J.-Q. Zhang, W. Zhang, H. Zhu, X.-G. Zhang, Chin. J. Explos. Propell. 29 (2006) 36–40.
[10] H.-Z. Li, Y. Huang, M. Huang, H. Dong, in: Y. Wang, P. Huang, S. Li (Eds.), Theory and Practice of Energetic Materials, vol. VI, Science Press, Beijing, China, 2005, pp. 149–151.
[11] H.-Z. Li, M. Huang, J.-H. Zhou, M. Shen, Y. Chen, Q. Peng, Energetic Mater. (China) 14 (2006) 381–384.
[12] G.D. Solodyuk, M.D. Boldyrev, B.V. Gidaspov, V.D. Nikolaev, Zh. Org. Khim. 17 (1981) 861–865.
[13] G.B. Belov, Propell., Explos., Pyrotech. 23 (1998) 86–89.
[14] R.W. Beal, M.S. Thesis, University of Delaware, 2000, 101 pp.
[15] V.P. Sinditski, S.P. Smirnov, V.Yu. Egorshev, Propell., Explos., Pyrotech. 32 (2007) 277–287.
[16] Yu.Ja. Maksimov, in: K.K. Andreev (Ed.), Theory of Explosives, Vysshaya Shkola, Moscow, 1967, pp. 73–84.
[17] V.P. Sinditskii, W.D. He, V.V. Serushkin, A.E. Fogelzang, A.B. S Sheremetev, Proceedings of the 29th International Annual Conference of ICT, Paper 170, Karlsruhe, FRG, 30 June–July 3, 1998, pp. 1–11.
[18] G.B. Manelis, G.M. Nazin, Yu.I. Rubtsov, V.A. Strunin, Thermal Decomposition and Combustion of Explosives and Pouders, Nauka, Moscow, 1996, 82–87 (in Russian).
[19] D.R. Stull, E.F. Westrum, G.C. Sinke, The Chemical Thermodynamics of Organic Compounds, John Wiley and Sons, Inc., 1969.
[20] Y.B. Zeldovich, Zh. Eksperimentalnoy i Teoreticheskoi Fiziki (Russ. J. Exp. Theor. Phys.) 12 (1942) 498–524.
[21] S. Patai (Ed.), The Chemistry of Hydrazo, Azo and Azoxy Groups (The Chemistry of Functional Groups), Wiley and Sons, London, 1975.
[22] J.H. Teles, G. Maier, Chem. Ber. 122 (1989) 745–748.